Numerical Simulation of Temperature Distribution during Short Pulse Laser Processing of Aluminum Thin Films

HASSANEEN JABBAR ABD
Department of mechanical engineering(power), College of engineering University of Karblaa, Iraq
hassaneen78@yahoo.com phone: 07801745756

ABSTRACT:

Fourier equation does not accurately predict the transient temperature during microscale laser heating of thin films. Therefore, non-Fourier behaviors may be significant for such microscale applications as pulsed-laser processing of metal and semiconductors, thin-film applications, and even laser surgery. A numerical model is developed to represent the temperature distribution during ultra short pulsed laser processing of aluminum thin films. The model developed is based on the solution of non-Fourier heat conduction problem with different thermal fluxes using explicit finite differences method. A computer program Quick-Basic language was built to perform the solution. The results of Non-Fourier heat conduction equation were compared with the results of Fourier heat conduction equation and showed that when the time increased Non-Fourier equation will be Fourier equation. The results showed that when increased the heat flux greater than $10^9 W$ the problem convert from one-dimensional non-Fourier heat conduction to one-dimensional non-Fourier phase change.

الخلاصة

معادلة فورير لايمكنها التنبوء بدقة لدرجات الحرارة ألانتقاليه أثناء التسخين ليزر صغير الحجم من الأغشية الرقيقة. ولذلك, سلوكيات لافورير قد تكون كبيرة مثلا تطبيقات صغيرة الحجم عمليات تصنيع المعادن وأشباه الموصلات بنبضات الليزر, تطبيقات الأغشية الرقيقة, وحتى عمليات الليزر. نموذج عددي تم تطويره لتمثيل توزيع درجات الحرارة لطبقة رقيقة من الألمنيوم أثناء نبضة ليزرية قصيرة جدا. النموذج المطور يستند على حل معادلة لافورير للتوصيل الحراري لمختلف التدفقات الحرارية باستخدام طريقة الفرو قات المحددة الصريحة. تم بناء برنامج حاسوبي بلغة الكوك بيسك لاحتضان الجانب النظري . نتائج معادلة لافورير للتوصيل الحراري تم مقارنتها مع نتائج فورير للتوصيل الحراري وظهر انه عندما يزداد الزمن معادلة لافورير تصبح فورير. النتائج بينت انه عندما نزيد الفيض الحراري عن $10^9 W$ المسالة تتحول من لافورير أحادي البعد إلى لا فورير متغير الطور.

Key words: non-Fourier, heat conduction, short pulse laser.

Nomenclature:

The following symbols are used generally throughout the text. Other are defined as when used:

C: Thermal Wave Speed(*m/sec*).
c_p: Specific Heat at Constant Pressure(*J/Kg.* C°).
i: Time Direction(-).
j: The Index Increment Along the Distance(-).
K: Thermal Conductivity(*W/m.* C°).
L: Thickness of thin film*(m)*.
M: Number of Time Step(-).
N: Total Number of Spatial Nodes(-).
q: Heat Flux(W/m^2).
Q: Constant Heat Flux(W/m^2).
t: Time*(sec)*.
T: Temperature(C°).
o:Initial(-).
X:Distance*(m)*.
α: Thermal Diffusivity(m^2/sec).
ρ: Density(kg/m^3).
τ : Relaxation Time*(sec)*.
μ :Micron(10^{-6}).

1-INTRODUCTION:

The most widely used equation governing heat propagation in isotropic homogenous media is Fourier's law of heat conduction:

$$q = -k\nabla T \qquad \textbf{(1)}$$

Where q is the local heat flux across a surface, k is the local thermal conductivity of the media, and ∇T is the local gradient of temperature T in the media. The energy equation for a rigid material with no volumetric energy supply is:

$$\rho c_p \partial_t T = -\nabla \cdot q \qquad \textbf{(2)}$$

Where ρ is the material density, c_p is the specific heat capacity, ∂_t is the partial differential operator with respect to time t, and $\nabla \cdot q$ is the divergence of the heat flux. When Fourier's law **(1)** is substituted into the energy equation **(2)** for a homogeneous material with constant material properties, Fourier's heat equation is obtained:

$$\partial_t T = \alpha \nabla^2 T \qquad \textbf{(3)}$$

Where

$$\alpha = \frac{k}{\rho c_p} \qquad \textbf{(4)}$$

Where α is the thermal diffusivity of the material and ∇^2 is the spatial Laplacian operator.
At high energy density beam sources, such as electron or laser beam, can produce extremely short pulse, high peak frequencies, and high heat flux, which are widely used in material processing**[1]**. For example, in electron beam penetration welding, for heat flux in the order of $10^7 to 10^9 \, W/cm^2$, the surface heating moves inwards very rapidly. Heating rates are $10^{10} - 10^{12}$ much faster than conventional method, such as arc welding. Even though Fourier's heat equation **(3)** is an excellent model for many heat transfer problems, the model is not physically realistic. Equation **(3)** is a parabolic equation. As a result, any temperature disturbance will propagate at an infinite speed through the media **[2]**. Thus, using equation **(1)** results in thermal waves traveling at an infinite speed, which is physically unrealizable**[3].** Because Fourier's law does not predict finite wave speeds, the law does not accurately approximate the heat transfer in certain cases. The assumption of instantaneous energy transmission fails during a short duration of an initial transient, or when the thermal propagation speed is not high, such as in low temperature cases **[2].** In other words, Fourier's law breaks down at temperatures near absolute zero or when the observation time is extremely small during a transient. For these cases, the fact that thermal disturbances travel with finite speeds of propagation must invalidate Fourier's law **(1)**. Thus, the wave nature of thermal transport becomes dominant, rendering Fourier's law to be invalid as an approximation for these cases **[4].**

Non-Fourier heat conduction models have been proposed to replace models based on Fourier's law. Specifically, non-Fourier models have been designed to predict ***second sound*** in solids, which is the finite wave speed of heat propagation **[5].** One Non-Fourier model is based on the modified flux law**[6]**:

$$q+\tau\frac{\partial q}{\partial t}=-k\nabla T \tag{5}$$

Where τ is called the ***relaxation time*** **[2]**. The heat flux vector now has a memory that keeps track of the time-history of the temperature gradient **[6]**. Equation **(5)** was first proposed independently by Cattaneo **[7]** and Vernotte **[8].**

When equation **(5)** is combined with the energy equation **(2)**, the hyperbolic heat conduction equation is obtained:

$$\tau\partial_t^2 T+\partial_t T=\alpha\nabla^2 T \tag{6}$$

Equation **(6)** is known as a hyperbolic heat equation **(or a telegraph equation)** because of the additional term that modifies the parabolic Fourier heat equation **(3)** **[7]**. The hyperbolic heat equation has two double-derivative terms in **(6).** which are called the wave terms. Unlike Fourier's law **(1),** the modified heat flux equation**(5)** predicts a finite speed of heat propagation because of the relaxation time **(τ)** associated with heat transfer **[7].** In fact, it can be shown that the speed C of heat propagation is :

$$C=\sqrt{\alpha/\tau} \tag{7}$$

2-Mathematical Model:

Mostly heat conduction problems involving simple geometries with simple boundary conditions had been considered because only such simple problems can be solved analytically. But many problems encountered in practice involving complicated geometry with complex boundary conditions or variable properties cannot be solved analytically. In such case, sufficiently accurate approximate solutions can be obtained by computers using a numerical method.

Non-Fourier heat conduction equation can be solved analytically by using Laplace transformation or numerically by using finite differences methods, finite elements methods, boundary elements methods, finite strips methods, and collocations methods. In this work finite differences methods used to solve the governing equations of non-Fourier heat conduction in thin film of aluminum initially at the equilibrium reference temperature T_o. At t=0, the external surface at x=0 is suddenly exposed to the short pulsed of laser and the case shown in the figure(1). The heat flux is all absorbed on the surface with no heat being lost to the surroundings.

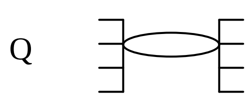

Figure(1): shows the case of study

The governing differential equation represented by the hyperbolic heat conduction equation(8) for temperature distribution, and non-Fourier equation for heat flux distribution (9).

$$\frac{1}{c^2}\frac{\partial^2 T}{\partial t^2}+\frac{1}{\alpha}\frac{\partial T}{\partial t}=\frac{\partial^2 T}{\partial x^2} \tag{8}$$

And

$$q + \tau \frac{\partial q}{\partial t} = -k \nabla T \qquad \textbf{(9)}$$

Many initial and boundary conditions are used to find the temperature distribution of hyperbolic heat conduction equation, , heat flux distribution. The initial and boundary conditions for Non-Fourier heat conduction are:

$$\left.\begin{array}{l} T = T_{\circ} \\ \dfrac{\partial T}{\partial t} = 0 \\ q(x,0) = 0 \end{array}\right\} \text{at } t = 0, x > 0 \qquad \textbf{(10)}$$

And

$$\left.\begin{array}{l} q(0,t) = Q \\ -k \dfrac{\partial T(0,t)}{\partial x} = \tau \dfrac{\partial q(0,t)}{\partial t} + q(0,t) \end{array}\right\} \qquad \textbf{(11)}$$

and

$$\left.\begin{array}{l} \dfrac{\partial T(L,t)}{\partial x} = 0 \\ q(L,t) = 0 \end{array}\right\} \qquad \textbf{(12)}$$

3-Numerical Formulation:

The mesh of the case study shown in figure(2).

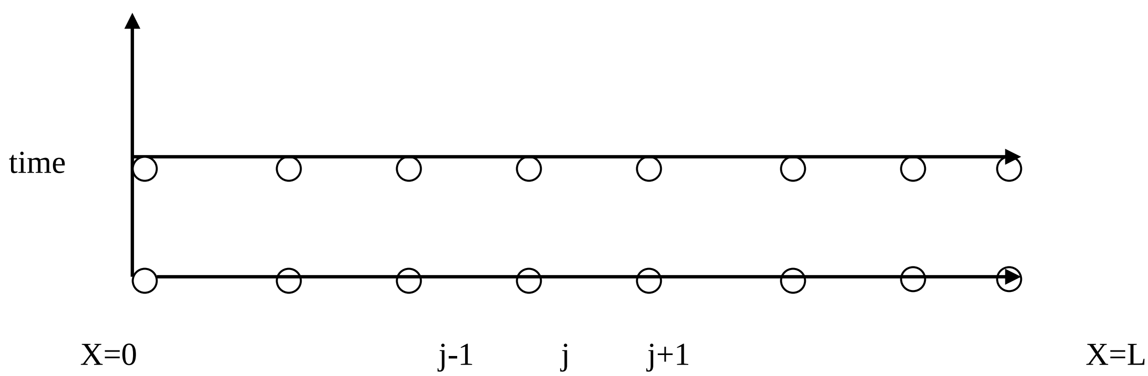

Figure(2): shows the mesh of the case study

The spatial Explicit Finite Difference Method will be used to solved the hyperbolic heat conduction equation(8), and Cattaneo-Vernott equation(9) as.

$$\tau \left[\frac{T_j^{i+1} + T_j^{i-1} - 2T_j^i}{\Delta t^2} \right] + \frac{T_j^{i+1} - T_j^i}{\Delta t} = \alpha \frac{T_{j+1}^i + T_{j-1}^i - 2T_j^i}{\Delta x_{(j)}^2} \qquad \textbf{(13)}$$

After rearranging equation (13) the following equation is obtained,

$$T_j^{i+1} = \frac{1}{1+\Delta t/\tau}\left[-T_j^{i-1} + T_j^{i}(2+\frac{\Delta t}{\tau} - 2\lambda_3) + \lambda_3(T_{j+1}^{i} + T_{j-1}^{i})\right] \qquad \textbf{(14)}$$

Where:

$$\lambda_3 = \frac{\alpha \Delta t^2}{\tau \Delta x_{(j)}^2} \qquad \textbf{(15)}$$

After substituting the initial condition (10) we get,

$$T_j^{i+1} = \frac{1}{2+\Delta t/\tau}\left[T_j^{i}(2+\frac{\Delta t}{\tau} - 2\lambda_3) + \lambda_3(T_{j+1}^{i} + T_{j-1}^{i})\right] \qquad \textbf{(16)}$$

From the boundary condition (12) at x=0 we get,

$$T_\circ^{i+1} = \left[T_1^{i+1} + \frac{\Delta x_{(1)}\tau}{k\Delta t}(q_0^{i+1} - q_0^{i}) + \frac{\Delta x_{(1)}}{k\tau} q_0^{i}\right] \qquad \textbf{(17)}$$

Substitute the boundary condition $x = L$ (12) in (14) to get,

$$T_N^{i+1} = \frac{1}{1+\Delta t/\tau}\left[-T_N^{i-1} + T_N^{i}(2+\frac{\Delta t}{\tau} - 2\lambda_3) + \lambda_3(T_{N-1}^{i} + T_{N-1}^{i})\right] \qquad \textbf{(18)}$$

Substituting equation (12) in equation (16) to get,

$$T_N^{i+1} = \frac{1}{2+\Delta t/\tau}\left[T_N^{i}(2+\frac{\Delta t}{\tau} - 2\lambda_3) + \lambda_3(T_{N-1}^{i} + T_{N-1}^{i})\right] \qquad \textbf{(19)}$$

The heat flux distribution is found by solving equation (9),

$$\tau\left[\frac{q_j^{i+1} - q_j^{i}}{\Delta t}\right] + q_j^{i} = -k\frac{T_{j+1}^{i} - T_j^{i}}{\Delta x_{(j)}} \qquad \textbf{(20)}$$

After rearranging equation (20) we get,

$$q_j^{i+1} = q_j^{i}(1-\frac{\Delta t}{\tau}) - \frac{\Delta t k}{\tau \Delta x_{(j)}}(T_{j+1}^{i} - T_j^{i}) \qquad \textbf{(21)}$$

At $x = 0$ the boundary condition is equation (11) and at $x = L$ is (12)

4-Results and Discussion:

Aluminum distribution contains temperature distribution, and heat flux distribution first should know the properties of AL and the parameters:

$(\tau = 10^{-12}, L = 10^{-5}\,m, \alpha = 8.418\times10^{-5}\, m^2/\sec, k = 204\,W/m.C^\circ, \rho = 2707\,kg/m^3, c_p = 0.896\,kJ/kg.C^\circ)$,

$(Q = 10^8 W, 10^9 w)$ and $(t_{\max} = 30 picosecond, pico = 10^{-12} second)$

Figures. from (a) to (h) show the temperature distribution of an Aluminum thin film subjected to a constant heat flux plotted against the distance for various values of time. Figures from (a) to fig.(b) for $Q = 10^8 W$, and figures from (c) to (f) for $Q = 10^9 W$ predict the propagation of thermal waves traveling through the medium at a finite speeds of heat propagation. The discontinuity predicted by the non-Fourier heat conduction is due to this finite speed. Fig.(c) for $Q = 10^8 W$, and fig.(g) for $Q = 10^9 W$ shown that the thermal wave is reflected back to the medium which causes an increase in the temperature distribution profile which take place when time greater than $(3*10^{-12})$. The reason of reflected thermal wave is the isolated end of the Aluminum medium. In fig.(d) Aluminum reached to the steady state, and at this heat flux $(Q = 10^8 W)$ the Aluminum is heating only but, in fig.(h) the Aluminum reached to the steady state at heat flux $(Q = 10^9 W)$ the Aluminum is melting. when increased the heat flux greater than $10^9 W$ the problem convert from one-dimensional non-Fourier heat conduction to one-dimensional non-Fourier phase change.

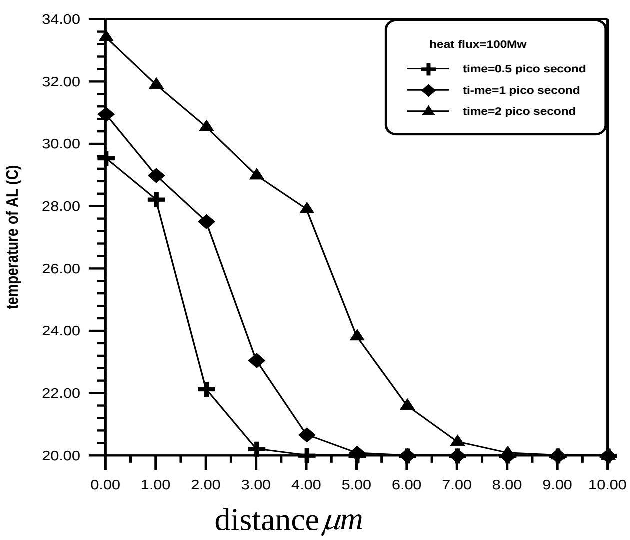

(a)

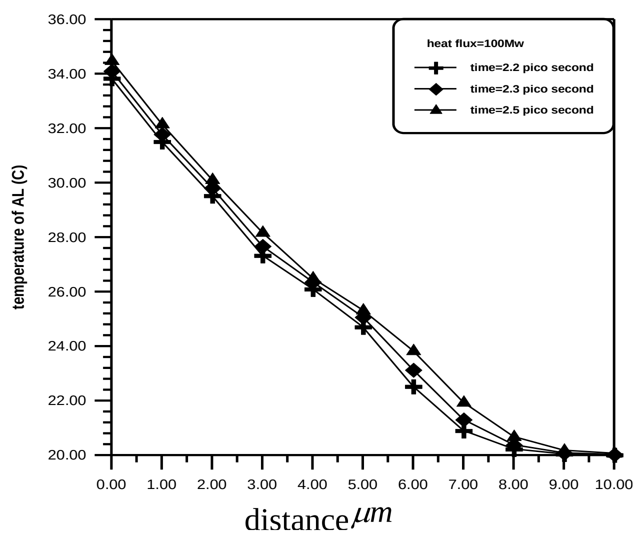

(b)

Figures(a)to(b): Shows Temperature Distribution in a Finite Medium Subjected by Constant Heat Flux.

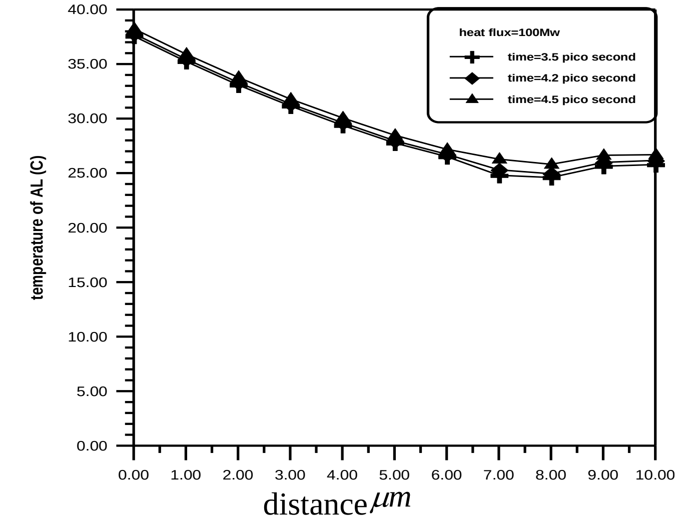

(c)

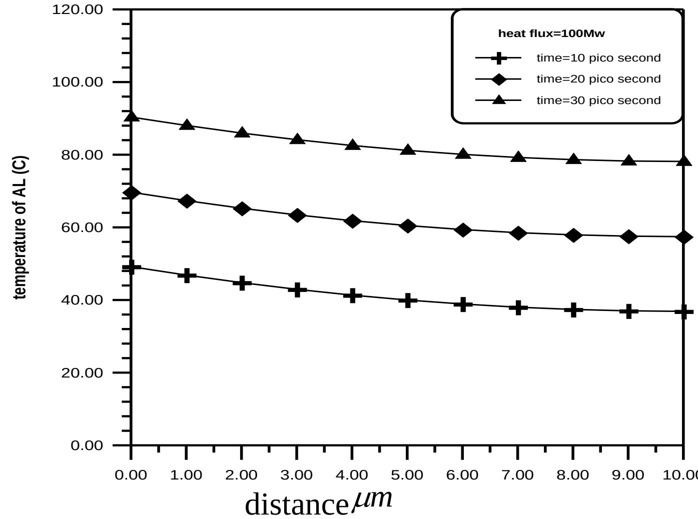

(d)

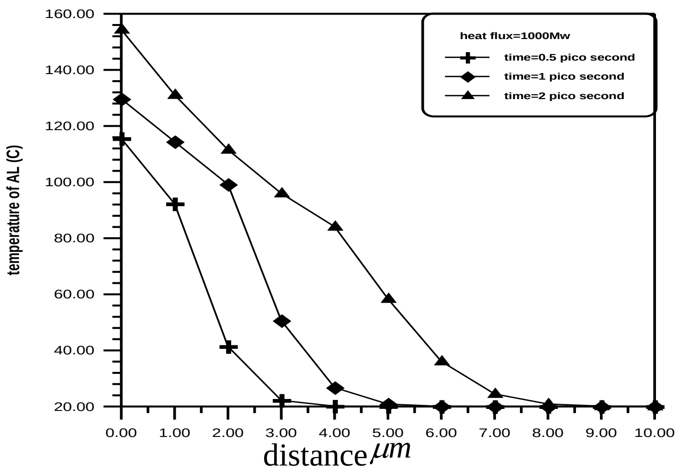

(e)

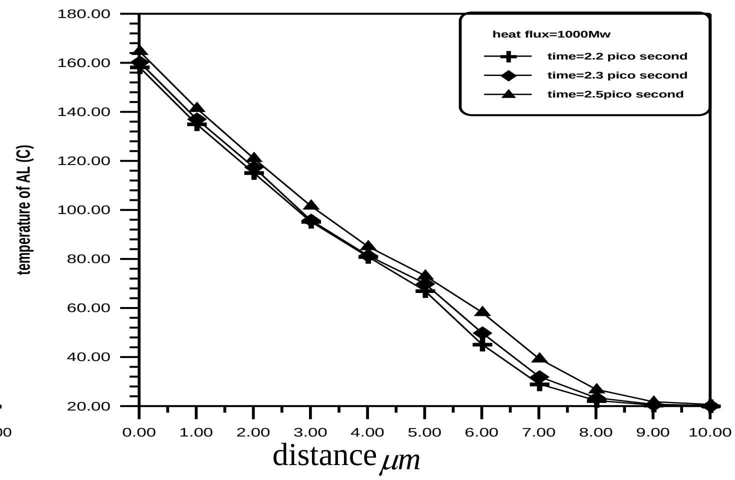

(f)

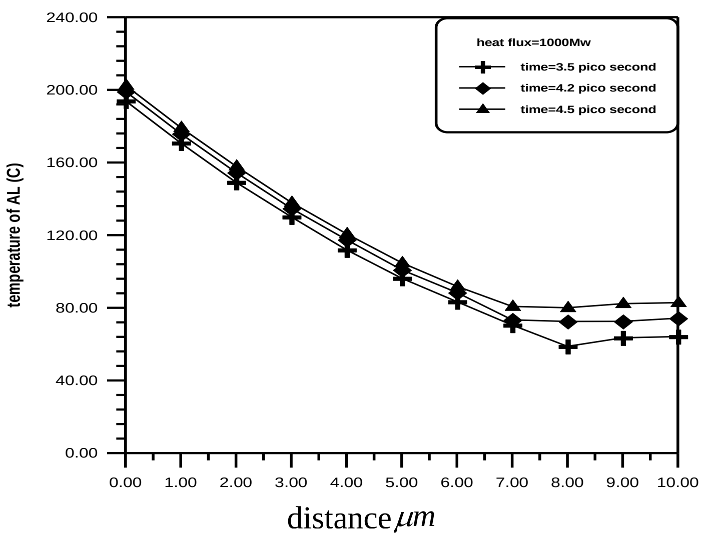

(g)

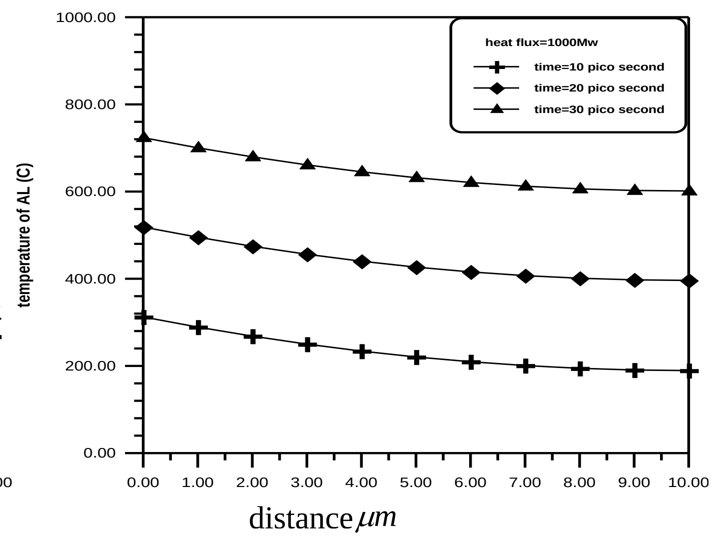

(h)

Figures(c)to(h): Shows Temperature Distribution in a Finite Medium Subjected by Constant Heat Flux.

Figures from **(a)** to **(h)** show the variation of heat flux of Aluminum with distance for various values of time in thin film subjected to a constant heat flux $(10^8 W, 10^9 W)$. At $x = 0$, its noticed that the heat flux is the greater for all values of time (the input heat flux at the left end). In all figures the wave nature of heat flux is noticed due to the finite speed of heat propagation. The figures explain that along the medium $x > 0$, the heat flux is increased with increasing of time due to the accumulation effect of the heat flux . When the values of time are greater than $(3*10^{12}\ \sec ond)$ the heat flux wave reflected from the right-hand side which causes an increase in heat flux and this shown in fig.(c) for $Q = 10^8 W$, and fig.(g) for $Q = 10^9 W$.

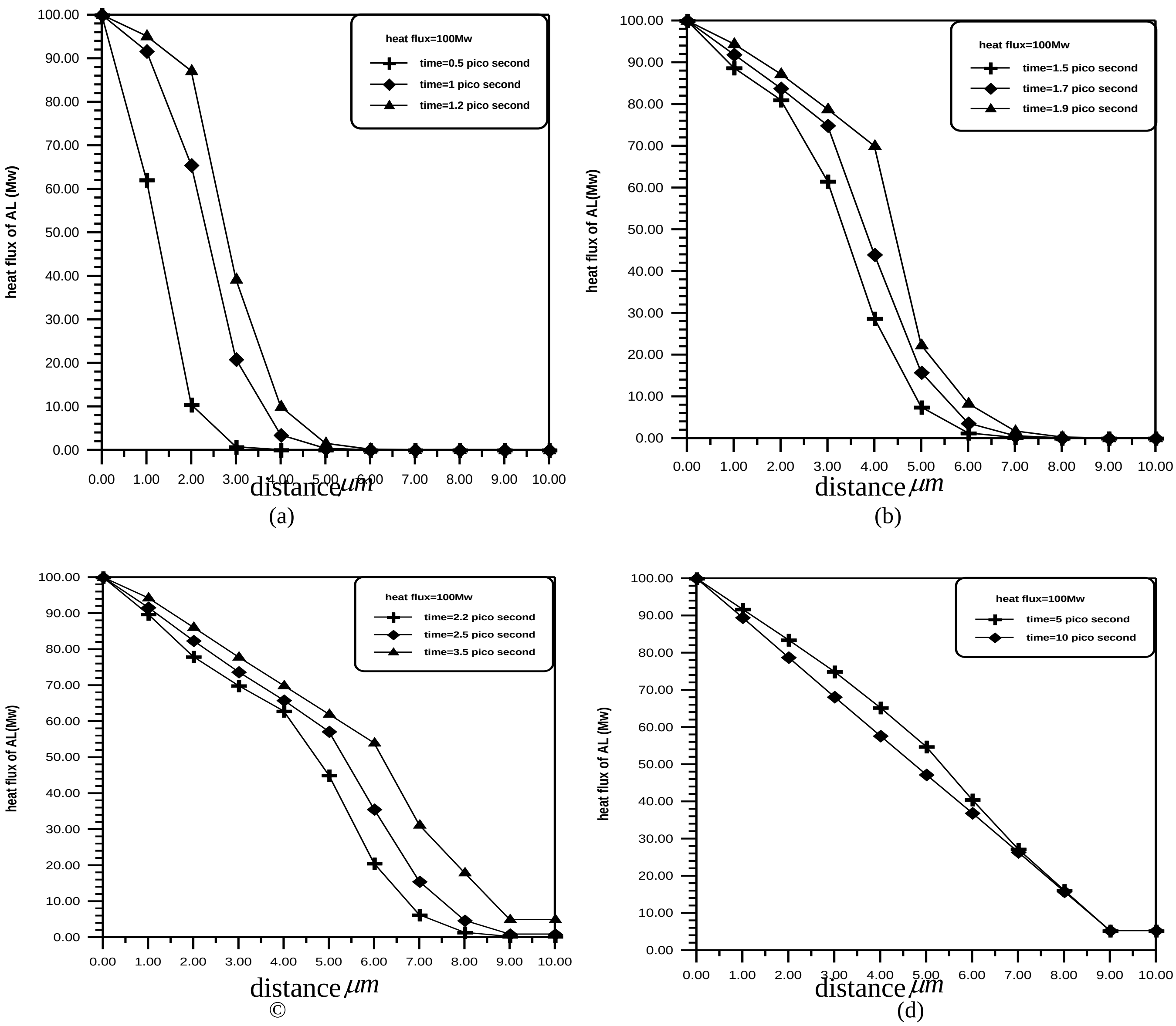

Figures(a) to(d): Shows The Variation of Non-Dimensional Heat Flux with Non-Dimensional Distance in a Finite Medium Subjected to a Constant Heat Flux.

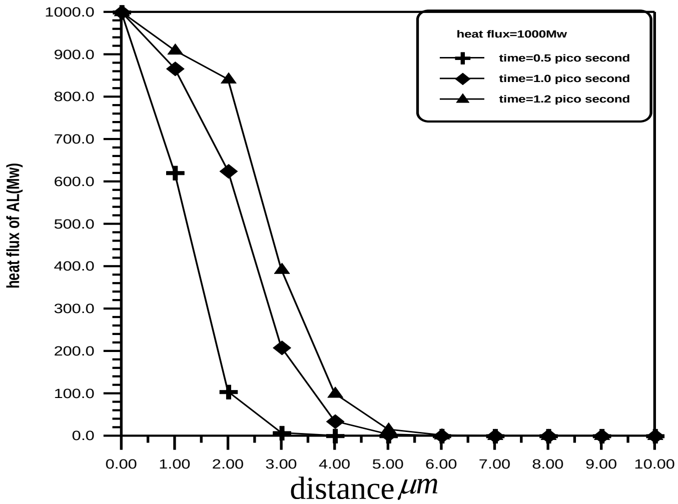

(e)

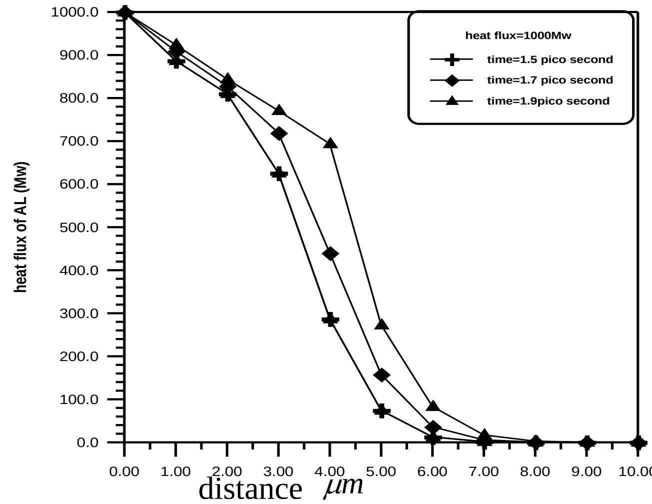

(f)

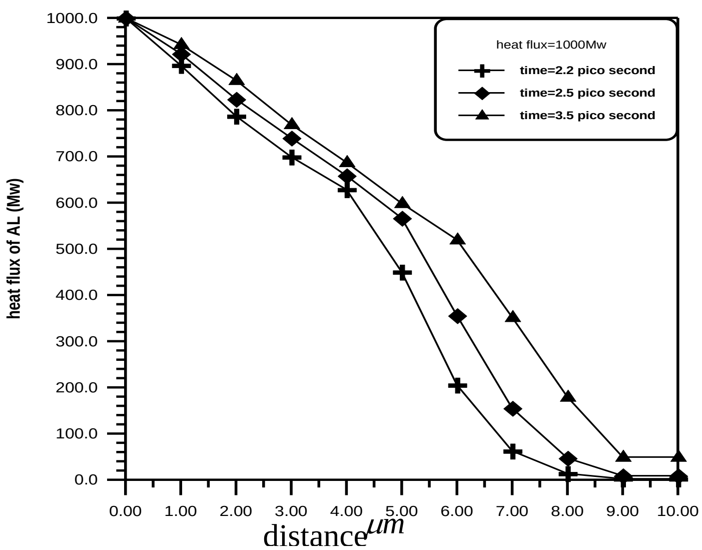

(g)

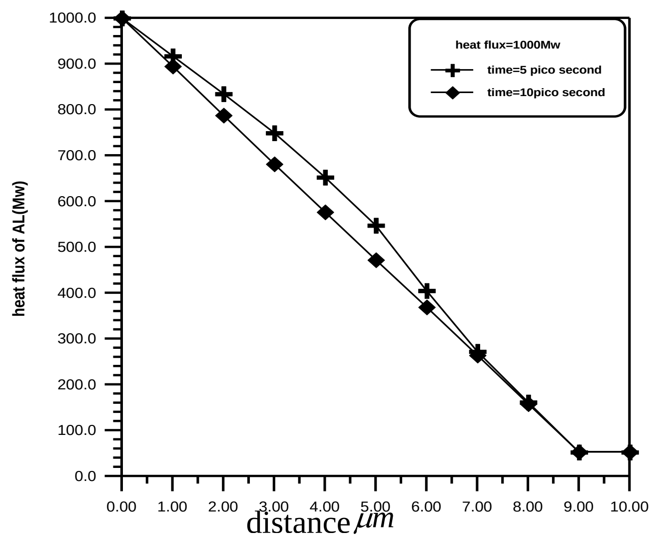

(h)

Figures(e)to(h): Show The Variation of Non-Dimensional Heat Flux with Non-Dimensional Distance in a Finite Medium Subjected to a Constant Heat Flux.

References:

[1]- Maurer, M. J., Thompson, H. A., "**Non-Fourier effects at high heat flux**", ASME J. of Heat Transfer, Vol.95, pp.284-286,1973.

[2]- Antaki, P.J., "**Solution for Non-Fourier Dual Phase Lag Heat Conduction in a Semi-Infinite Slab With Surface Heat Flux**", Int.J.Heat Mass Transfer, Vol.41, No.14, pp.2253-2258,1998.

[3]- Glass, D.E.,Ozisik, M.N., and McRae, D.S., "**On the Numerical Solution of Hyperbolic Heat Conduction**", Numerical Heat Transfer, Vol.8, pp.497-504,1985.

[4]- Herwing, H., and Beckert, k., "**Fourier Versus Non-Fourier Heat Conduction in Materials With a Nonhomogenous Inner Structure**", J.Heat Transfer,Vol.122, pp.363-365,2000.

[5]- Qiu, T.Q., and Tien, C.L., "**Heat Transfer Mechanisms During Short-pulse Laser Heating of Metals**", J. Heat Transfer, Vol.115, pp.835-841,1993.

[6]- Tang, D.W., and Araki, N., "**Non-Fourier Heat Conduction in a Finite Medium Under Periodic Surface Thermal Disturbance**", Int.J.Heat Mass Transfer, Vol.39, No.8, pp.1585-1590,1996.

[7]- Vedavarz, A., Kumar, s., and Moallemi, M.K., "**Significance of Non-Fourier Heat Waves in Conduction**", J.Heat Transfer, Vol.116, pp.116-224,1994.

[8]- Yang, H.Q., "**Non-Fourier Effect on Heat Conduction During Welding**", Int.J.Heat Mass Transfer, Vol. 34, No.11, pp.2921-2924,1991.